Magnetic anisotropy strength and surface alloy formation in Mn/Co/Cu(001) overlayers

B.-Ch. Choi, P. J. Bode, and J. A. C. Bland
Cavendish Laboratory, Madingley Road, Cambridge CB3 0HE, United Kingdom
(Received 28 July 1998)

The correlation between the structure and magnetic properties of ultrathin Mn overlayers grown on fcc Co/Cu(001) was studied using low-energy electron diffraction and the magneto-optic Kerr effect *in situ*. A two-dimensional magnetic $c(2\times2)$ Mn-Co(001) surface alloy was found to be stabilized in the range 0.3–0.8 ML Mn overlayer thickness. Within this thickness range Mn is ferromagnetically coupled to the fcc Co(001) underlayer. Above one monolayer of Mn, the $c(2\times2)$ surface reconstruction fully disappears and the Mn overlayers are no longer ferromagnetically ordered. Furthermore, it is shown that the Kerr signal, magnetic anisotropy strength, and coercivity are correlated with the stabilization of the MnCo surface alloy and growth conditions. [S0163-1829(99)02709-5]

I. INTRODUCTION

The effect of nonmagnetic overlayers on the magnetic coupling and magnetic anisotropy behavior at ferromagnetic interfaces is an important issue.[1–4] Much attention has been recently given to studies of the structure and magnetism of two-dimensionally (2D) ordered surface alloys based on transition metals, since they provide important insights into the effects of the adsorbed nonmagnetic atoms on the magnetic ordering in ultrathin magnetic films.[5,6] A wide range of Mn surface alloys, based on Mn/Cu(001), Mn/Ni(001), and Mn/Fe(001),[6–9] have been studied theoretically and experimentally, both because of a rich variety of possible structural and magnetic phases occurring in epitaxially grown Mn films and because a large magnetic moment can form due to the half-filled *3d* shell of Mn. An interesting feature of the Mn-based surface alloys is the formation of the thermodynamically stable $c(2\times2)$ superstructure, which has been observed by Wuttig *et al.*[10] in the MnCu surface alloy on Cu(001). Such 2D surface alloys provide possibilities for the preparation of the very stable ultrathin films in the monolayer range and enable the experimentalist to perform well-controlled experiments to verify the theoretical predictions. The Mn/Co/Cu(001) structure provides a model epitaxial system which is well suited to the study of the magnetic coupling of the Mn adatoms to the ferromagnetic Co underlayer. Experimentally, O'Brien and Tonner[11] have used x-ray magnetic circular dichroism to infer that a single Mn monolayer is ferromagnetically aligned with respect to the fcc Co(001) film. On the other hand, a competition between an in-plane antiferromagnetically ordered $c(2\times2)$ configuration and one in which a ferromagnetic Mn monolayer is antiferromagnetically coupled with respect to the Co underlayer is predicted by tight-binding model calculations.[9] In this context it is important to note that any minor perturbation in the actual unit-cell structure can have a potentially major influence on the magnetic properties given that the structural and magnetic energy contributions to the total energy are comparable in magnitude.

In the present paper, we report the results of a careful study of the influence of Mn overlayers on the structural and magnetic properties of fcc Co/Cu(001). The stabilization of a 2D $c(2\times2)$ MnCo magnetic surface alloy was found within a Mn overlayer thickness range of 0.3–0.8 ML, where Mn is aligned ferromagnetically with respect to the fcc Co/Cu(001). Moreover, it will be shown that the stabilization of the $c(2\times2)$ MnCo surface alloy is clearly correlated with the long-range magnetic ordering of Mn atoms at the Mn/Co interface, and that the change in the magnetic properties resulting from the structural change sensitively controls the magneto-optic response and coercivity.

II. EXPERIMENT

Experiments were performed *in situ* in ultrahigh vacuum (UHV) with a base pressure of $\sim1\times10^{-10}$ mbar. The fcc Co(001) surfaces were prepared at room temperature by molecular-beam epitaxy onto a Cu(001) single crystal at an evaporation rate of 1 ML/min. The Cu substrate is slightly miscut [$\sim0.5°$ off the (001) normal direction], and therefore the step direction runs along the [100] direction. Throughout the experiment 8–9 ML of Co layers were deposited, because the Co film growth proceeds in a layer-by-layer growth mode above 2 and up to 10 ML,[12,13] and no substrate Cu-atom diffusion was found after 6 ML of Co deposition.[13,14] The Co film thickness was determined by Auger electron spectroscopy. The low-energy electron diffraction (LEED) pattern obtained after the deposition of 8–9 ML Co showed still sharp (1×1) spots, indicating that Co grows pseudomorphically on the Cu(001) surface. Thereafter, Mn overlayers up to 4 ML thickness have been deposited on the fcc Co(001) surface at room temperature. The Mn evaporation rate was calibrated by monitoring the $c(2\times2)$ LEED pattern formed at $\frac{1}{2}$ ML coverage of Mn on Cu(001).[10] The formation of the MnCo surface alloys was observed by an ordinary LEED system. Magnetic properties were investigated using *in situ* magneto-optical Kerr effect (MOKE) in the transverse geometry, applying magnetic fields along the [110] and [100] directions, respectively.

III. EXPERIMENTAL RESULTS AND DISCUSSION

In the initial stage of Mn growth on the fcc Co(001) surface, the Mn grows epitaxially adopting the in-plane spacing

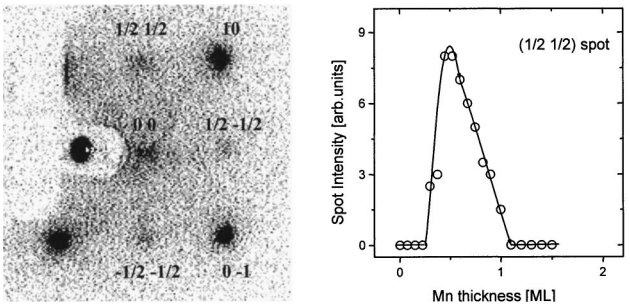

FIG. 1. (a) $c(2\times2)$ LEED pattern for 0.5 ML of Mn on fcc Co(001), measured at 136 eV. The intensities of the $c(2\times2)$ superstructure spots are very faint. (On the left-hand side of the photo the shadow of the sample holder and the LEED electron gun are also seen.) (b) Normalized LEED intensities of the $(\frac{1}{2})$ $(\frac{1}{2})$ beam in $c(2\times2)$ superstructure as a function of Mn thickness. The solid line is guide to the eye.

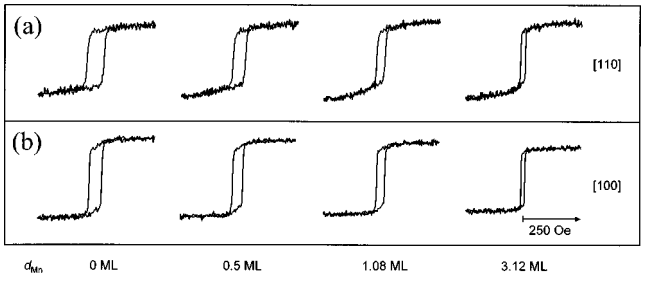

FIG. 2. *M(H)* Hysteresis loops obtained during the growth of the Mn overlayer onto the 8 ML fcc Co/Cu(001) structure at 300 K. The applied magnetic field was aligned along the [110] direction [the magnetic easy axis of the ideal Co/Cu(001) (Ref. 11)] in Fig. 2(a) and the [100] direction (45° from the [110] axis) in the Fig. 2(b), respectively. The relative loop heights correspond to the experimentally observed signals.

and symmetry of fcc Co(001), and a sharp (1×1) LEED pattern was formed. When the Mn overlayer is thicker than ~0.3 ML, faint half-order spots appear in addition to the integer-order spots. With increasing Mn coverage the superstructure beams become more intense. In Fig. 1(a) we show a diffraction pattern at 136 eV obtained from 0.5 ML Mn on Co/Cu(001). We attribute this $c(2\times2)$ superstructure to the formation of the ordered MnCo surface alloy, which is consistent with the stabilization of the CuMn surface alloy after deposition of ~0.5 ML Mn on the Cu(100) surface.[10,15] In principle, however, other mechanisms might be responsible for generating extra spots in the present system. First, the interdiffusion of substrate Cu atoms through the Co film might lead to the formation of a MnCu surface alloy. This possibility can be ruled out because the substrate interdiffusion can be neglected for Co layers above 6 ML thicknesses.[13] In support of this view, the formation of the MnCo surface alloy is found to correlate directly with the long-range ferromagnetic order in the Mn/Co/Cu(001) system, whereas the MnCu surface alloy was found to show no long-range magnetic order at room temperature.[10] This point will be discussed later in detail. The second possible mechanism is related to the formation of an antiferromagnetic superstructure, as predicted by Tamura, Blügel, and Feder.[16] However, the extra spot intensities in a single antiferromagnetic layer are expected to be much weaker than we observed. In fact, the ratio of the $(\frac{1}{2}\ \frac{1}{2})$ spot intensity maxima was measured to be about 20% of the (00) spot intensity, which is a factor of at least 10 times larger than the generally expected value of ~2% for the antiferromagnetism-induced reconstruction.[16] Consequently, the above two mechanisms can be ruled out.

In order to understand the formation of the MnCo surface alloy, the intensity of the extra spots in the $c(2\times2)$ LEED pattern was measured and the background intensity subtracted. In Fig. 1(b) we plot the $(\frac{1}{2}\ \frac{1}{2})$ extra spot intensity as a function of Mn thickness. A careful search using LEED revealed no detectable extra spots in the submonolayer Mn thickness range. The minimum Mn coverage at which the $c(2\times2)$ structure is observable is found to be ~0.3 ML. As Mn grows further a maximum intensity of the $(\frac{1}{2}\ \frac{1}{2})$ beam was found at ~0.5 ML, denoting that the 2D $c(2\times2)$ MnCo surface alloy is best ordered at this coverage. This is in a good agreement with the previous scanning tunneling microscopy (STM) result of the MnCu surface alloy,[17,18] showing that the ordering of the incorporated Mn atoms into a $c(2\times2)$ structure starts at around 0.3 ML Mn and is completed at 0.5 ML Mn. With further deposition of Mn the $c(2\times2)$ spot intensity decreases, indicating that after 0.5 ML deposition the Mn atoms no longer become incorporated into the $c(2\times2)$ structure, and finally disappears after deposition of a monolayer of Mn. Therefore, above 0.5–1 ML Mn there exists a coexistence of those of the Mn atoms incorporated in a $c(2\times2)$ structure and those adsorbed on the alloy surface. This result is consistent with the result of Wuttig *et al.*,[19] reporting that only the first layer of MnCu is alloyed. A rough estimate of the surface roughness can be obtained from the spot profile analysis of the (10) and $(\frac{1}{2}\ \frac{1}{2})$ spots. At a primary beam energy of 136 eV we found that the half width of the (10) spot increases with Mn deposition, indicating an increase of the surface roughness with increasing Mn overlayer thickness. At 0.5 ML Mn thickness, the half widths of the (10) and $(\frac{1}{2}\ \frac{1}{2})$ spots are found to be of the same magnitude (~12% of the surface Brillouin zone along the [100] direction), indicating that the coherence lengths for $c(2\times2)$ and (1×1) long-range order are comparable in magnitude.

Figure 2 presents hysteresis loops obtained *in situ* during the growth of the Mn overlayer onto the 8 ML fcc Co/Cu(001) structure at room temperature. The applied field was aligned along the [110] direction [the magnetic easy axis of the ideal Co/Cu(001)] in Fig. 2(a) and along the [100] direction in Fig. 2(b), respectively. We first observe that *M(H)* loops in the [110] direction are not fully square, in contrast to the usual easy magnetization behavior for the Co/Cu(001) system, where fcc Co has a large in-plane fourfold anisotropy and its easy axes lie along the {110} crystallographic directions.[4] This indicates that the magnetic easy axis of the fcc Co(001) departs from the fourfold [110] easy axis. *M(H)* loops in the [100] direction for the uncovered Co are also nearly square and fully saturated at 250 Oe. As the field is reduced from the saturation value to zero the magnetization rotates with respect to the [100] axis and there is a gradual decrease of the MOKE signal from saturation followed by an abrupt magnetization switch until negative saturation is reached. Thus we conclude that a strong in-plane uniaxial anisotropy is superimposed on the fourfold magne-

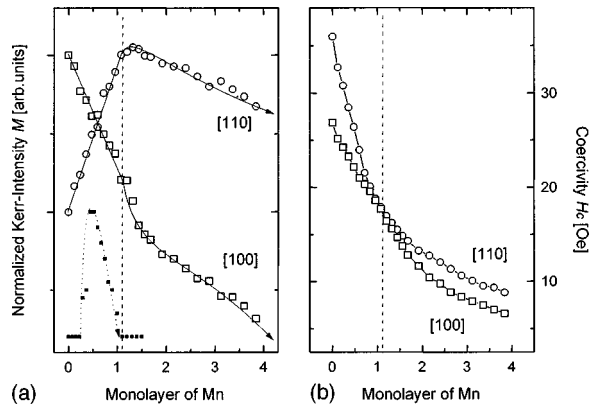

FIG. 3. The behavior of (a) the Kerr intensity M measured for an applied field strength of 250 Oe and (b) the coercive field H_c as a function of the Mn thickness with the field applied along the [110] and [100] directions, respectively. The M values are normalized to the M value obtained in the uncovered 8 ML Co film. The thickness dependent $c(2\times2)$ spot intensity (the dotted line) in Fig. 2 is also given to emphasize the correlation between the Kerr signal and the formation of the $c(2\times2)$ surface alloy. The lines are guides to the eye. The vertical dashed line divides the region with and without the $c(2\times2)$ surface reconstruction.

tocrystalline anisotropy for the uncovered 8 ML Co/Cu(001) film. The uniaxial anisotropy is attributed to the step-induced anisotropy which results from the slight miscut ($\sim$0.5°) of the Cu substrate, where the surface steps are aligned along the [100] direction. Hence, the reduced symmetry at steps introduce additional twofold contributions to the effective anisotropy. Such a uniaxial contribution was distinctly demonstrated by Krams and co-workers[20,21] in Co films grown on vicinal surfaces. With further deposition of Mn overlayers, the shape of the *M(H)* loops in the [110] direction develop towards two-step loops, as clearly identified above 0.5 ML of Mn, whereas the loop shapes in the [100] direction do not change significantly within the investigated thickness range. A more quantitative evaluation can be deduced from the analysis of the hysteresis loops.

We now address the issue of how the stabilization of the MnCo surface alloy correlates with the magnetic structure in the Mn/fcc Co(001) system. Figure 3 shows the evolution of (a) the loop amplitude M measured for an applied field strength of 250 Oe and (b) the coercive field H_c as a function of Mn overlayer thickness, along the [110] and [100] directions, respectively. The magnetic properties change clearly, indicating a very sensitive response to submonolayer coverages of Mn. For the Kerr-signal $M_{[110]}$ projected along the [110] direction, a monotonic increase is found for coverages up to $\sim$1 ML Mn with an enhancement of the order of 10% at 0.8 ML Mn [Fig. 3(a)]. This indicates that the deposited Mn layers are all ferromagnetically ordered with respect to the Co underlayer, which is consistent with the experimental result by O'Brien and Tonner using XMCD,[11] where they found that a monolayer Mn is ferromagnetically ordered and magnetically aligned with the fcc Co(001) underlayer. More importantly in our measurement, the Mn thickness region for which ferromagnetic coupling of Mn to the Co occurs explicitly corresponds to the coverage where the $c(2\times2)$ surface reconstruction is found to be stabilized. Above 1 ML of Mn, the Kerr-signal $M_{[110]}$ begins to fall, indicating that additional Mn atoms above one monolayer are no longer ferromagnetically ordered. In the observed nonferromagnetic phase of Mn, no $c(2\times2)$ superstructure was found and the (1×1) spots remain. From this correlation we conclude that the ferromagnetic coupling is associated with only those Mn atoms which are either directly incorporated into the $c(2\times2)$ structure or which are in proximity with Co atoms as is the case for the additional Mn atoms deposited up to a coverage of 1 ML. The Mn atoms are in both cases ferromagnetically aligned with the Co layer, but the Mn atoms which begin to agglomerate with further deposition of Mn above 1 ML are not ferromagnetically aligned. Supporting this idea, it was reported by O'Brien and Tonner[11] that the Mn surface layer is ferromagnetically ordered when Mn is in direct contact with the ferromagnetic fcc Co(001) substrate. Also relevant is the prediction[9] that the coupling between Mn and a fcc Co(001) underlayer is strongly dependent on Mn coverage. Surprisingly, different behavior for the Kerr-signal $M_{[100]}$ was found in the [100] direction, where $M_{[100]}$ decreases gradually with increasing Mn coverage. The reduction in $M_{[100]}$ seen in the Mn thickness range 0–1 ML suggests that strong changes in the magneto-optic response may be occurring as has been reported previously for submonolayer coverage of nonmagnetic metal on Co.[4] Alternatively, the magnetic configuration of the Mn may depend on the direction of the applied magnetic field during Mn growth.

To understand the above M behavior, it is important to distinguish between the anisotropic contributions of Mn atoms adsorbed on two different kinds of binding sties on the Co surface, e.g., terrace sites and step edges, which might prefer different magnetic anisotropies. From the $c(2\times2)$ surface reconstruction revealed in the LEED pattern [Fig. 1(a)] we postulate that the energetically favorable adsorption sites of Mn atoms are terrace sites, where the incorporation of Mn atoms into the $c(2\times2)$ structure occurs. This hypothesis is supported by the STM study of the ordering of the MnCu surface alloy by Flores and co-workers,[17,18] where a $c(2\times2)$ structure is clearly visible on the terrace and on the islands at 0.45 ML Mn on a Cu(001) substrate [Fig. 2(a) of Ref. 18]. Therefore, the thickness dependence of the Kerr-signal M in Fig. 3(a) is interpreted as follows; initially the deposited Mn atoms are bound predominantly on the terrace sites, not at the step edges, and Mn atoms at the terrace sites play a dominant role in the ferromagnetic coupling of Mn atoms to the Co underlayer. This is physically reasonable since the symmetry around Mn atoms in terrace sites is fourfold giving rise to a fourfold magnetocrystalline anisotropy, whereas Mn atoms on step edges have a reduced symmetry leading to a uniaxial magnetic anisotropy. The variation in anisotropy strength is correlated with concurrent variation in the magneto-optic response. Supporting this view, we note that the Kerr signals M for both directions exhibit sharp turning points at a coverage of one monolayer [Fig. 3(a)], which is clearly associated with the stabilization of the magnetic MnCo surface alloy. As more Mn is grown above 1 ML, the Mn overlayers are no longer ferromagnetically ordered. Thus the Kerr signal in both directions ($M_{[110]}$ and $M_{[100]}$) decreases gradually as the magnetic layer is progressively buried by the nonmagnetic Mn overlayer.

Further experimental evidence for the influence of the magnetic anisotropy on the magnetic properties is the varia-

tion of the coercivity H_c with Mn coverage, shown in Fig. 3(b) for both directions. The coercivity H_c is found to decrease continuously with increasing Mn thickness. As expected, the evolution of H_c is clearly dependent on Mn coverage. Interestingly, the values of H_c in the thickness range between 0.7 and 1 ML Mn were identical in both directions, which cannot be explained in a direct way from our measurements since for the interpretation of the change in H_c many factors such as domain formation could be involved. The evolution of H_c in Fig. 3, however, clearly demonstrates that the change in H_c is directly correlated with that of *M.* Both M and H_c reveal significant changes at the Mn coverage of $\sim$1 ML (denoted by a vertical dashed line), which divides the two different structural regions for Mn overlayers with and without the presence of the $c(2\times2)$ surface reconstruction. From these results we conclude that the magnetization and coercivity are linked, and therefore that the main mechanism for the change of M and H_c is either the strong response of the magneto-optical signal to small changes in the surface structure induced by the stabilization of the surface alloy or a field induced magnetic configuration in the Mn during growth in the submonolayer range.

IV. CONCLUSION

In conclusion, we found a striking sensitivity of the surface structure and magnetic properties in ultrathin fcc Co/Cu(001) structures to the deposition of submonolayers of Mn. The magnetic properties correlate directly with the stabilization of a two-dimensional $c(2\times2)$ MnCo surface alloy. Corresponding to the two structural regions defined by the absence and stabilization of the surface alloy respectively, two magnetic phases of Mn overlayers were identified; a ferromagnetic phase due to interfacial coupling up to a monolayer of Mn, and a nonmagnetic phase above 1 ML of Mn. We conclude that the Kerr-signal, magnetic anisotropy strength and coercivity are correlated with the stabilization of the MnCo surface alloy and growth conditions.

ACKNOWLEDGMENTS

The financial support of the Engineering and Physical Sciences Research Council (EPSRC) and the British Council Alliance programs are gratefully acknowledged. We thank C. Demangeat for helpful discussions.

[1] W. Weber, C. H. Back, A. Bischof, D. Pescia, and R. Allenspach, Nature (London) **374**, 788 (1995).
[2] J. A. C. Bland, S. Hope, M. Tselepi, and B.-Ch. Choi, J. Phys. D **31**, 622 (1998).
[3] S. Hope, E. Gu, B.-Ch. Choi, and J. A. C. Bland, Phys. Rev. Lett. **80**, 1750 (1998).
[4] F. O. Schumann, M. E. Buckley, and J. A. C. Bland, J. Appl. Phys. **76**, 6093 (1994).
[5] B.-Ch. Choi, P. J. Bode, and J. A. C. Bland, Phys. Rev. B **58**, 5166 (1998).
[6] W. L. O'Brien and B. P. Tonner, Phys. Rev. B **51**, 617 (1995).
[7] H. A. Dürr, G. van der Laan, D. Spanke, F. U. Hillebrecht, N. B. Brookes, and J. B. Goedkoop, Surf. Sci. **377**, 466 (1997).
[8] J. Dresselhaus, D. Spanke, F. U. Hillebrecht, E. Kisker, G. van der Laan, J. B. Goedkoop, and N. B. Brookes, Surf. Sci. **377**, 450 (1997).
[9] A. Noguera, S. Bouarab, A. Mokrani, C. Demangeat, and H. Dreysse, J. Magn. Magn. Mater. **156**, 21 (1996).
[10] M. Wuttig, Y. Gauthier, and S. Blügel, Phys. Rev. Lett. **70**, 3619 (1993).
[11] W. L. O'Brien and B. P. Tonner, Phys. Rev. B **50**, 2963 (1994).
[12] H. Li and B. P. Tonner, Phys. Rev. B **40**, 10 241 (1989).
[13] M. T. Kief and W. F. Egelhoff, Phys. Rev. B **47**, 10 785 (1993).
[14] J. J. de Miguel, A. Cebollada, J. M. Gallego, R. Miranda, C. M. Schneider, P. Schuster, and J. Kirschner, J. Magn. Magn. Mater. **93**, 1 (1991).
[15] R. G. P. van der Kraan and H. van Kempen, Surf. Sci. **338**, 19 (1995).
[16] E. Tamura, S. Blügel, and R. Feder, Solid State Commun. **65**, 1255 (1988).
[17] T. Flores, S. Junghans, and M. Wuttig, Surf. Sci. **371**, 1 (1997).
[18] T. Flores, S. Junghans, and M. Wuttig, Surf. Sci. **371**, 14 (1997).
[19] M. Wuttig, C. C. Knight, T. Flores, and Y. Gauthier, Surf. Sci. **292**, 189 (1993).
[20] P. Krams, B. Hillebrands, G. Güntherodt, and H. P. Oepen, Phys. Rev. B **49**, 3633 (1994).
[21] P. Krams, F. Lauks, R. L. Stamps, B. Hillebrands, G. Güntherodt, and H. P. Oepen, J. Magn. Magn. Mater. **121**, 483 (1993).